

MACHINE DESIGN E061322: COMPUTATIONAL ASSIGNMENT

| | |
|--------------------|---|
| Case Study | Computational Modelling of the lubricated Piston-Ring Cylinder-liner contact in an IC Engine |
| Supervisor | Prof. Dieter Fauconnier |
| Groups | Maximum 3 persons |
| Competences | <ul style="list-style-type: none"> · Being able to adequately collect, analyse and summarize relevant scientific and technical information related to mechanical systems and processes. · Understanding the principles of advanced mechanical design and lubrication. · Analysis of mechanical components and systems with respect to durability and reliability. · Work in a team. |
| Evaluation | <ul style="list-style-type: none"> · Group report & simulation files to be submitted on Ufora by December 31st. · Accounts for 40% of the total course score. |

CONTEXT

Piston rings are split rings that fit into a groove on the piston-head mantle. These components are crucial to guarantee normal operation and good performance in internal combustion (IC) engines. Their main functions are:

1. Sealing the combustion chamber and prevent combustion gas leakage to the crank case.
2. Guiding and supporting the reciprocating sliding movement of the piston, by sustaining a lubricant film.
3. Regulating the amount of lubricant between the piston and the cylinder wall, controlling lubrication and engine oil consumption.
4. Improving heat transfer from the piston to the cylinder wall.

Piston rings may account for 34%-45% of the total friction in internal combustion engines.¹ This considerable contribution is a result of the compromise needed to achieve performant sealing while reducing friction and wear. Sealing and oil regulation are achieved by multiple rings, each with their own function, using a metal-on-metal sliding contact.

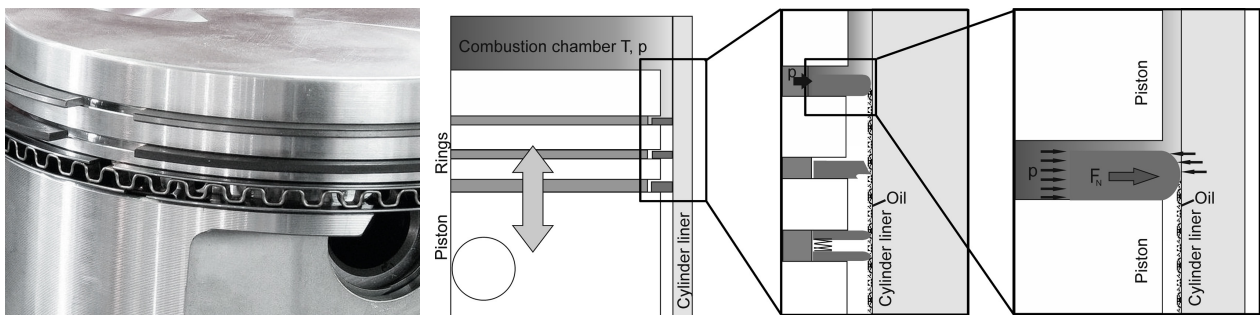


Figure 1: Due to the high pressures, the compression ring is forced down to the lower surface of the piston groove and pushes the ring radially outward to the cylinder liner, where the compressed oil film provides the sealing

¹Shahmohamadi, H., Rahmani, R., Rahnejat, H., Garner, C.P., King, P.D., 2013. Thermo-Mixed Hydrodynamics of Piston Compression Ring Conjunction. Tribology Letters 51, 323-340.

Four stroke Diesel Engines typically have three rings as shown in Figure 1:

1. The top ring, or **Compression Ring**, must deliver consistent compression sealing to maximize power output and control “blow-by”, gases to the carter. Typical compression ring designs will have an essentially rectangular cross section with a barrel-shaped top profile.
2. The second ring, or **Scraper Ring** is intended to remove oil from the cylinder wall and prevent it from entering the combustion chamber, and typically has a taper napier form.
3. The bottom ring, or **Oil Control Ring**, consists of an expander ring and two rails which control the supply of oil to the liner and returning it to the crankcase via small drain-back slots in the rear wall of the oil ring grooves.

Lubrication of piston rings is particularly complex as the rings have an oscillating motion. At the limits of piston movement, the ring stops and reverses direction, which disrupts the normal oil wedge effect in hydrodynamic lubrication regime, potentially leading to wear on both the cylinder liner as the piston ring. Furthermore, the radial load on the compression ring varies with the crank angle ψ . Indeed, during the suction and exhaust strokes, a relatively low atmospheric pressure prevails in both the combustion chamber and the carter (by approximation). However, during the compression and expansion strokes, the pressure of the working fluid in the combustion chamber varies with the crank angle ψ . Due to the high pressures, the compression ring is forced down to the lower surface of the piston groove and pushes the ring radially outward to the cylinder liner, where the compressed oil film provides the sealing (Figure 1). This implies that the pressures at the inlet/outlet of the oil film are different and that also the hydrodynamic pressure in the oil film must increase or decrease according to the compression ring load determined by the combustion chamber pressure.

The objective(s) of this assignment is to model, investigate and understand the lubricated contact physics of the compression ring during its reciprocating unsteady motion in the cylinder. Thereto a numerical simulation tool must be written in either Python which allows to calculate the hydrodynamic lubricant film between the cylinder liner and the compression ring, taking into account all boundary effects as well as the temperature dependency of the lubricant.

PHYSICAL DESCRIPTION

Current assignment investigates the compression-ring liner system of the Volkswagen Golf Mk6 Diesel Engine VW 2.0 R4 16v TDI CR 105kW – 141 bhp @ 4.200 rpm; 320 newton metres @ 1.750-2.500 rpm – for which all needed technical details are enlisted in Table 1 in the appendices. The required oil for this type of engine is the multi-grade oil SAE 5W-40. The nominal oil temperature is 95°C. Table 2 in the appendix gives an overview of all thermo-mechanical properties of the lubricant, including some empirical or physics-based relations as function of operating pressure and temperature.

The physical model of the compression-ring-cylinder-liner system is elaborated below

KINEMATICS

First a kinematic analysis is required to describe the reciprocating motion of the piston within the cylinder which will define the pressure-build up beneath the sliding compression ring. Using the notation in Figure 2 (left), the position of the piston head, its velocity and the acceleration are expressed as function of the crank angle ψ , the crank length R_c and the connecting rod length l_r as

$$y(t) = R_c \cos(\psi) + l_r \cos(\alpha) \quad (1)$$

$$\dot{y}(t) = -R_c \dot{\psi} \sin(\psi) - l_r \dot{\alpha} \sin(\alpha) \quad (2)$$

$$\ddot{y}(t) = -R_c \ddot{\psi} \sin(\psi) - R_c \dot{\psi}^2 \cos(\psi) - l_r \ddot{\alpha} \sin(\alpha) - l_r \dot{\alpha}^2 \cos(\alpha) \quad (3)$$

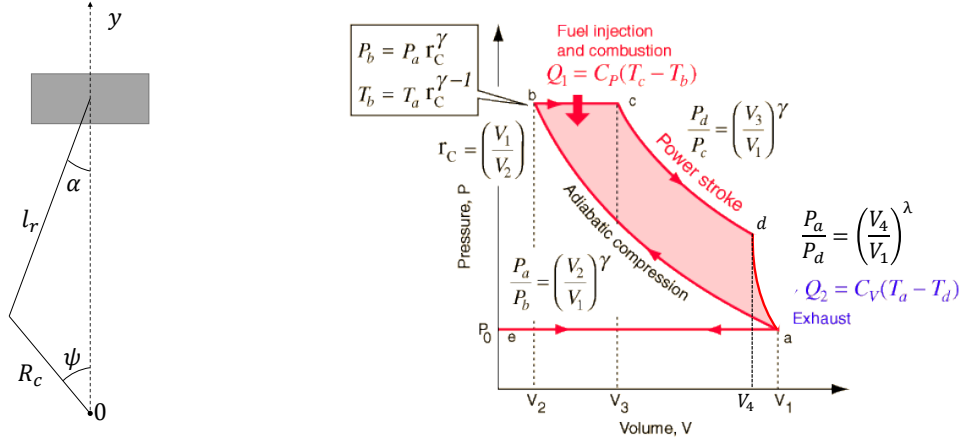


Figure 2: Piston Kinematics (right) and thermo-dynamic diesel cycle (left)

in which

$$\alpha = \arcsin \left(\frac{R_c}{l_r} \sin(\psi) \right) \quad (4)$$

$$\dot{\alpha} = \frac{R_c \dot{\psi} \cos(\psi)}{l_r \cos(\alpha)} \quad (5)$$

$$\ddot{\alpha} = \frac{R_c - \dot{\psi}^2 \sin(\psi) + \ddot{\psi} \cos(\psi)}{l_r \cos(\alpha)} + \dot{\alpha}^2 \tan(\alpha) \quad (6)$$

Assuming a constant angular velocity ω , the crank angle ψ , and its derivatives are defined as

$$\psi = \omega t \quad (7)$$

$$\dot{\psi} = \omega \quad (8)$$

$$\ddot{\psi} = 0 \quad (9)$$

The Internal volume of the cylinder with diameter D as function of crank angle $\psi = \omega t$ is defined as

$$V(\psi) = V_{min} + \frac{\pi D^2}{4} (R_c + l_r - y(\psi)) \quad (10)$$

in which V_{min} is the minimum cylinder volume i.e. in the top dead centre (TDC), and is calculated from the stroke length $S = 2R_c$ and the compression ratio CR as

$$V_{min} = \frac{\pi D^2}{4} \frac{S}{CR - 1} \quad (11)$$

The maximum cylinder volume is then given by

$$V_{max} = V_{min} CR \quad (12)$$

The sliding distance s of the piston head over time t can be calculated numerically as

$$s(t) = \int_0^t \sqrt{1 + \dot{y}^2} dt \quad (13)$$

COMBUSTION PRESSURE

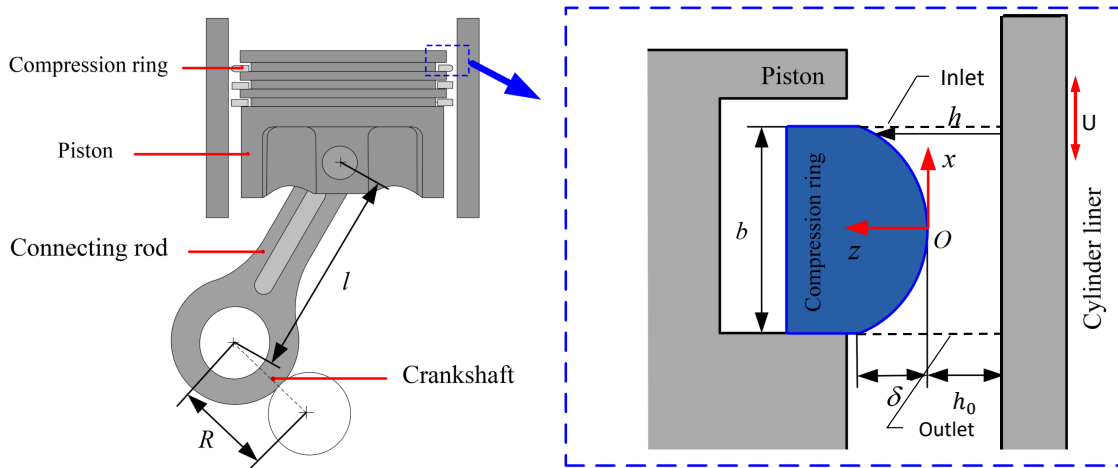
As explained in the introduction the pressure-build up in the lubricant film also depends on the combustion chamber pressure which determines the radial/normal load on the compression ring. Therefore, it is crucial to describe properly the combustion chamber pressure by assuming adiabatic compression and expansion in e.g. the idealized diesel cycle as depicted in Figure 2 (right). The pressure in the combustion chamber p_{cc} is given as function of the crank angle ψ as

$$\frac{p_{cc}(\psi)}{p_a} = \begin{cases} 1 & 0 \leq \psi < \psi_{IVC} \quad \text{Intake} \\ \left(\frac{V_{max}}{V(\psi)}\right)^\gamma & \psi_{IVC} \leq \psi < \psi_{SOC} \quad \text{Adiabatic Compression} \\ CR^\gamma & \psi_{SOC} \leq \psi < \psi_{EOC} \quad \text{Isobaric Combustion} \\ CR^\gamma \left(\frac{V(\psi_{EOC})}{V(\psi)}\right)^\gamma & \psi_{EOC} \leq \psi < \psi_{EVO} \quad \text{Adiabatic Expansion} \\ \left(\frac{V_{max}}{V(\psi)}\right)^k & \psi_{EVO} \leq \psi < 3\pi \quad \text{Isochoric Expansion} \\ 1 & 3\pi \leq \psi \leq 4\pi \quad \text{Blow Out} \end{cases} \quad (14)$$

in which angle at intake valve closure ψ_{IVC} , angle at start of combustion ψ_{SOC} , angle at end of combustion ψ_{EOC} and angle at exhaust valve opening ψ_{EVO} . The isochoric expansion coefficient k is obtained as

$$k = \frac{\ln(p_{cc}(\psi_{EVO})/p_a)}{\ln(V_{max}/V(\psi_{EVO}))} \quad (15)$$

REYNOLDS EQUATION



The lubrication film in the piston-ring cylinder-liner contact is governed by the 1D Reynolds equation in combination with a 1D temperature equation. Consider the local coordinate system $x \in [-\frac{b}{2}, \frac{b}{2}]$. The Reynolds equation then reads

$$\frac{\partial}{\partial x} \left(\phi \frac{\partial p}{\partial x} \right) = \frac{U}{2} \frac{\partial \rho h}{\partial x} + \frac{\partial \rho h}{\partial t}, \quad \phi = \frac{\rho h^3}{12\mu} \quad (16)$$

subject to Boundary Conditions

$$p\left(-\frac{b}{2}\right) = p_{carter} = 0 \quad (17)$$

$$p\left(\frac{b}{2}\right) = p_{cc}(\psi) - p_a \quad (18)$$

The film thickness h in Reynolds' equation is described as:

$$h(x) = h_0(\psi) + 4\frac{\delta x^2}{b^2} \quad (19)$$

whereas the sliding velocity of the cylinder liner is $U = -\dot{y}$. The algorithm with which to solve the Reynolds equation is given in Appendix.

TEMPERATURE EQUATION

For the temperature equation we consider only convective and conductive heat transfer in the lubricant film, whereas compressive heating is neglected. If the sliding velocity of the ring-liner contact is sufficiently large, the Péclet number $Pe > 1$, hence convective heat transfer will prevail. However, in the top and bottom dead centres, where the motion reverses, thermal conduction might play a role justifying the presence of this term. In order to minimize computational overhead, and since we are mainly interested in representative temperature, density and viscosity, which are averaged across the film a 1D temperature equation is considered (instead of 2D), in which shear heating and convective speed are evaluated by averaging over the film based. Hence, the equation for the mean temperature \bar{T} is defined as

$$\rho c_p \frac{\partial \bar{T}}{\partial t} + \rho c_p \bar{u} \frac{\partial \bar{T}}{\partial x} = \kappa \frac{\partial^2 \bar{T}}{\partial x^2} + \bar{Q} \quad (20)$$

Using the velocity profile

$$u(x, z) = \frac{1}{\mu} \frac{\partial p}{\partial x} \left(\frac{z^2 - h(x)z}{2} \right) - \frac{U}{h(x)} z + U, \quad (21)$$

we can work out the film-thickness averaged velocity \bar{u} and shear heating \bar{Q} , yielding

$$\bar{u} = \frac{1}{h} \int_0^h u(x, z) dz = -\frac{h^2}{12\mu} \frac{\partial p}{\partial x} + \frac{U}{2} \quad (22)$$

$$\bar{Q} = \frac{1}{h} \int_0^h \mu \left(\frac{\partial u}{\partial z} \right)^2 dz = \frac{h^2}{12\mu} \frac{\partial p^2}{\partial x} + \mu \frac{U^2}{h^2} \quad (23)$$

The temperature equation is then supplemented by following boundary conditions

$$U > 0 \quad \begin{cases} \frac{\partial T}{\partial x} \left(\frac{b}{2} \right) = 0 \\ T \left(-\frac{b}{2} \right) = T_{oil} \end{cases} \quad (24)$$

$$U \leq 0 \quad \begin{cases} T \left(\frac{b}{2} \right) = T_{oil} \\ \frac{\partial T}{\partial x} \left(-\frac{b}{2} \right) = 0 \end{cases} \quad (25)$$

The algorithm with which one can solve the temperature equation is discussed in the Appendix of this document.

CAVITATION MODEL

Defining α as a vapour volume fraction, we determine the density and viscosity of the homogeneous bubble-fluid mixture, i.e. lubricant - gas/vapour, as

$$\rho(p, T) = \rho_l (1 - \alpha) + \rho_v \alpha \quad (26)$$

$$\mu(p, T) = \mu_l (1 - \alpha) + \mu_v \alpha \quad (27)$$

$$c_p(p, T) = c_{p,l} (1 - \alpha) + c_{p,v} \alpha \quad (28)$$

The Lubricant properties, for both liquid and gaseous-vaporous phases are given in Table 2. For the sake of simplicity and numerical convergence, we adopt here a simple phenomenological description of the vapour volume fraction α as function of the absolute pressure (p), i.e.

$$\alpha(p) = \frac{1}{2} [1 + \tanh(\beta(p - p_0))] \quad (29)$$

in which coefficients β and p_0 are determined from imposing two target vapour volume fractions at saturation pressure p_s and vapour pressure p_v of the lubricant, i.e.

$$\alpha_s = 0.02 \leftrightarrow p_{absolute} = p_s \quad (30)$$

$$\alpha_v = 0.98 \leftrightarrow p_{absolute} = p_v \quad (31)$$

Hence, the coefficients β and p_0 yield

$$\beta = \frac{1}{2(p_s - p_v)} \ln \left(\frac{\alpha_s(\alpha_v - 1)}{\alpha_v(\alpha_s - 1)} \right) \quad (32)$$

$$p_0 = p_s - \frac{1}{2\beta} \ln \left(\frac{-\alpha_s}{\alpha_s - 1} \right) \quad (33)$$

FORCES

At each position of the piston ring, the load carrying capacity of the lubricated contact should be in equilibrium with the outward radial load on the compression ring due to elastic tension stresses of the ring and the pressure from the combustion chamber, i.e.

$$F_{elastic} + F_{compression}(\psi) = W_{hydrodynamic}(h_0(\psi)) + W_{asperities}(h_0(\psi)) \quad (34)$$

The radial force per unit length due to the elastic tension of the steel compression ring can be obtained according to following formula

$$F_{elastic} = \frac{16l_{gap,f}E_r I}{3\pi b D^4} b, \quad [N/m] \quad I = \frac{bw^3}{12}, \quad [m^4] \quad (35)$$

The radial force due to the combustion gasses working on the compression ring are given by

$$F_{compression} = (p_{cc}(\psi) - p_a) b \quad [N/m] \quad (36)$$

Solving Reynolds equation for the pressure, the hydrodynamic force per unit length is trivially calculated as

$$W_{hydrodynamic}(\theta) = \int_{-b/2}^{b/2} p(x) dx \quad [N/m] \quad (37)$$

The load carried by the interacting asperities during the mixed and boundary lubrication regime at e.g. piston reversal, is not trivial. Building upon the Greenwood-Williamson and Greenwood and Tripp² contact model for two nominally flat rough surfaces, Gore et al.³ modified this assumption, by taking into account the curvature of the barrel-shaped compression ring. Indeed, not all of the asperities in the contact area contribute to the load carrying capacity in the same way as the asperities located close to the contact centre. The contact model of Gore et al. applied to current

²Greenwood, James & H Tripp, J. (1970). The Contact of Two Nominally Flat Rough Surfaces. Archive: Proceedings of The Institution of Mechanical Engineers 1847-1982 (vols 1-196). 185. 625-634

³Gore, M., Morris, N., Rahmani, R., Rahnejat, H., King, P. D., and Howell-Smith, S. (2017) A combined analytical-experimental investigation of friction in cylinder liner inserts under mixed and boundary regimes of lubrication. Lubr. Sci., 29: 293– 316. doi: 10.1002/lis.1369

contact provides expressions for respectively the asperity load, real contact area of the asperity peaks, and the friction force due to the interacting asperities, as

$$W_{asperities} = \frac{16}{15} \sqrt{2\pi} (\zeta \kappa \sigma)^2 \sqrt{\frac{\sigma}{\kappa} E_{eq}} \sqrt{\frac{\sigma b^2}{4\delta}} \int_{\Lambda_0}^{\Lambda_c} F_{5/2}(\Lambda) \Lambda^{-1/2} d\Lambda \quad [N/m] \quad (38)$$

$$\frac{1}{E_{eq}} = \frac{1 - \nu_c^2}{E_c} + \frac{1 - \nu_r^2}{E_r} \quad (39)$$

$$A_{asperity} = \pi^2 (\zeta \kappa \sigma)^2 L \sqrt{\frac{\sigma b^2}{4\delta}} \int_{\Lambda_0}^{\Lambda_c} F_2(\Lambda) \Lambda^{-1/2} d\Lambda, \quad L = \pi D \quad [m^2] \quad (40)$$

$$F_{asperities} = \frac{\tau_0 A_{asperity}}{L} + f_b W_{asperities} \quad [N/m] \quad (41)$$

The underlying hypothesis for the expression of $F_{asperities}$ is that the asperities are wetted by adsorption of an ultra-thin film of boundary active molecules subject to non-Newtonian shear. This non-Newtonian shear behaviour commences at the Eyring shear stress of the lubricant, denoted by τ_0 . Furthermore f_b denotes the pressure coefficient of boundary shear strength of the softer of the two interfaces and can be regarded as a local coefficient of friction. Note that this contact model takes the dimensionless film thickness as an input, i.e.

$$\Lambda_0 = \min \left(\frac{h_0}{\sqrt{\sigma_c^2 + \sigma_r^2}}, \Lambda_c \right) \quad (42)$$

Λ_c denotes the critical dimensionless film thickness, for which the chance of direct asperity contact between a parabolic rough surface and a rough flat surface vanishes, and takes a value of $\Lambda_c = 2.2239$. The functions $F_{5/2}(\Lambda)$ and $F_2(\Lambda)$ are given by following analytical expressions

$$F_{5/2}(\Lambda) = \frac{1}{8\sqrt{\pi}} e^{-\frac{\Lambda^2}{4}} \Lambda^{\frac{3}{2}} \left((2\Lambda^2 + 3) \text{BesselK} \left(\frac{3}{4}, \frac{\Lambda^2}{4} \right) - (2\Lambda^2 + 5) \text{BesselK} \left(\frac{1}{4}, \frac{\Lambda^2}{4} \right) \right) \quad (43)$$

$$F_2(\Lambda) = \frac{1}{2} (\Lambda^2 + 1) \text{erfc} \left(\frac{\Lambda}{\sqrt{2}} \right) - \frac{1}{\sqrt{2\pi}} e^{-\frac{\Lambda^2}{2}} \quad (44)$$

in which *BesselK* denote modified bessel function of the second kind and *erfc* denotes the complementary error function. The integrals can be evaluated numerically in Python by making use of the built-in function *scipy.integrate.quad* in combination with functions.

LOAD BALANCE

The load equilibrium of equation (34) is satisfied for a unique value of the minimum film thickness $h_0(\psi)$. In order to find that value of the minimum film thickness h_0 for each crank angle ψ , we adopt the iterative **Quasi Newton-Raphson method or Secant method** to find the root of following error function which represents the load imbalance, i.e.

$$\Delta W = W_{hydrodynamic}(h_0) + W_{asperities}(h_0) - F_{elastic} - F_{compression}(\psi) \quad (45)$$

Hence, the film thickness on iteration $i + 1$ is obtained from previous data as

$$h_0^{i+1} = h_0^i - \theta \left[\frac{\Delta W(h_0^i)}{\Delta W(h_0^i) - \Delta W(h_0^{i-1})} \right] (h_0^i - h_0^{i-1}), \quad \forall i \geq 2 \quad (46)$$

in which $0 < \theta \leq 1$ is a user-defined under-relaxation factor to ensure stability of the procedure. In order to guarantee stability, it is advisable to impose $h_0^{i+1} \geq 0.1 \sqrt{\sigma_c^2 + \sigma_r^2}$ as additional safety

WEAR MODEL

In order to model the wear of the piston ring and the cylinder liner, we make use of Archard's Wear model, which states that the volume of material V_w which is lost due to wear is proportional to the work done by the friction forces. This is expressed as

$$V_w = k \frac{W_{Hertz}}{H} s, \quad [m^3] \quad (47)$$

in which k is the dimensionless wear coefficient, W_{Hertz} the normal load on the equivalent Hertz contact, H [Pa] the material hardness and s [m] the sliding distance.

This equation can also be written under its differential form for the **wear depth** h_w , as

$$dh_w = k \frac{p_{Hertz}}{H} ds, \quad [m] \quad (48)$$

The wear depth at the **centre area of the compression ring** is then given as function of the sliding distance by

$$h_{w,r}(s(t)) = k \int_0^{s(t)} \frac{p_{Hertz}(s(t))}{H_r} ds(t), \quad [m] \quad (49)$$

The wear depth at a **position x on the cylinder liner** is given as function of time by expression

$$h_{w,c}(x, t) = k \int_0^t \frac{p_{Hertz}(x(t)) U(x(t))}{H} dt, \quad [m] \quad (50)$$

The mean contact pressure p_{Hertz} at the nominal line contact is obtained using Hertz' expression as

$$p_{Hertz} = \frac{\pi}{4} \sqrt{\frac{W_{asperities} E_{eq}}{\pi R_{eq}}} \quad (51)$$

in which $W_{asperities} = W_{asperities}(h_0)$ denotes the film-thickness dependent asperity-load obtained from the Greenwood-Tripp asperity contact model.

ALGORITHM

The equations are solved using an computational algorithm that exists of 3 loops:

1. An outer loop to advance the solution in time
2. An intermediate loop that contains the iterative Quasi-Newton Method to satisfy the load balance per time step and determine the corresponding minimum film thickness h_0
3. An inner loop which iteratively solves the lubrication problem, i.e. Reynolds equation and temperature equation for a given minimum film thickness h_0 , by means of Picard iteration or fixed-point iteration

The outer and intermediate loops are combined in the main program (main.py) shown below in Algorithm 2, whereas Algorithm 1 describes the Reynolds-solver (ReynoldsSolver.py) containing the inner loop. Note that it is highly recommended to solve Reynolds equation and the Temperature equation in terms of absolute pressure and absolute temperature respectively, in order to have full consistency with the Equation of State and all Constitutive equations which rely on absolute state variables.

Algorithm 1: ReynoldsSolver.py

Function *Reynolds.SolveReynolds(StateVector,time)*

ReSet residual ε_P , ε_T and $k = 1$ **Calc** Mixture Density $\rho(x)$, Viscosity $\mu(x)$ & Specific Heat $c_p(x)$ on previous time-step $t - 1$ **while** ($\varepsilon_P > Tol_P$ or $\varepsilon_T > Tol_T$) and ($k < MaxIter$) **do**

1. **Calc** $\rho(P, T)$, $\mu(P, T)$, $c_p(P, T)$, and $\kappa(P, T)$ on current iteration
2. **Set** LHS of Reynolds' Equation
3. **Set** RHS of Reynolds' Equation
4. **Set** Pressure Boundary Conditions
5. **Solve** Linear System of Reynolds Equation **to** P^*
6. **Calc** $\Delta P = \max(P^*, 0) - P^k$
7. **Update** $P^{k+1} = P^k + \theta_P \Delta P$
8. **Set** LHS of Temperature Equation
9. **Set** RHS of Temperature Equation
10. **Set** Temperature Boundary Conditions
11. **Solve** Linear System of Temperature Equation **to** T^*
12. **Calc** $\Delta T = T^* - T^k$
13. **Update** $T^{k+1} = T^k + \theta_T \Delta T$
14. $k = k + 1$
15. Calculate residual $\varepsilon_P = \|\Delta P / (P^k)\| / N_x$
16. Calculate residual $\varepsilon_T = \|\Delta T / T^k\| / N_x$

end

Update Hydrodynamic Load, Wall Shear Stress, Viscous Friction Force in StateVector.

Algorithm 2: Main.py

Input:

1. Create an **Engine** object from the **EngineParts.py** class which stores the geometrical parameters and properties of the piston, cylinder, compression ring and valve timing.
2. Create an **Contact** object from the **TriboContact.py** class which provides information about the equivalent properties, roughness parameters and wear coefficients, along with the Greenwood-Tripp Asperity contact model and Wear model
3. Create a **Grid** object from the corresponding class to store computational mesh
4. Create a **Time** object to define and store the temporal discretization
5. Create a **Discretization** object from the **FiniteDifferences** class, providing the spatial discretization method, the finite difference operator matrices and the boundary condition routines
6. Create a **Ops** object to store the engine operating conditions, the engine kinematics and the cylinder pressure evolution during one combustion cycle
7. Create an **Oil** and **Vapour** object from the **Liquid** and **Gas** classes of the **FLuidLibrary.py** file, which defines all constitutive equations and equations of state.
8. Create an **Mixture** object from the **TwoPhaseModel.py** class, which defines the Cavitation model.
9. Create a list **StateVector** in which each member corresponds to a **State** object from the **State.py** class, storing all variables of interest at a given time step.
10. Create a **Reynolds** object from the **ReynoldsSolver.py** class in which the solution method for Reynolds and temperature equation is defined.

Initialize *StateVector* @ $t = 0s$;

Set *Maximum iterations, tolerances & under-relaxation factors for pressure, temperature and load balance solvers*;

while $t < t_{end}$ **do**

Update *time* $t=t+1$;

ReSet residual $\varepsilon_{h_0} = 1$, iteration $i = 1$;

Guess *Minimum film thickness h_0 , Pressure and Temperature based on the solution @ $t = t - 1$* ;

while $\varepsilon_{h_0}(i) > Tol$ & $k < MaxIter$ **do**

1. **Calc** Film Thickness Profile $h(x)$

2. **Calc** $\Lambda = h_0/\sigma$

3. **Calc** Asperity Contact Load: **Function** *Contact.AsperityContact(StateVector,t)*

4. **Calc** Hydrodynamic Load: **Function** *Reynolds.SolveReynolds(StateVector,t)*

5. **Calc** Load Balance: $\Delta W = W_{hydrodynamic}(h_0) + W_{asperities}(h_0) - F_{elastic} - F_{compression}(\psi)$

6. **Update** h_0 : $h_0^{k+1} = \max \left(h_0^k - \theta \left[\frac{\Delta W(h_0^k)}{\Delta W(h_0^k) - \Delta W(h_0^{k-1})} \right] (h_0^k - h_0^{k-1}), 0.1\sqrt{\sigma_c^2 + \sigma_r^2} \right)$

7. **Calc** Wear depth of both Cylinder and Ring.

8. **Update** All variables of interest in *StateVector*;

9. $k = k + 1$;

10. Calculate residual $\varepsilon_{h_0} = \left| \frac{h_0^k}{h_0^{k-1}} - 1 \right|$

end

end

ASSIGNMENT

1. Build in Python⁴ a computational model for the lubricated ring - liner contact, using the predefined template Python file structure enlisted below

| File/Class | Description |
|-----------------------------|--|
| Main.py | Overview in Algorithm 2 |
| ReynoldsSolver.py | Overview in Algorithm 1 |
| EngineParts.py | Geometry of Engine Components. |
| Ops.py | Operating Conditions, Engine Kinematics & Combustion Cycle |
| Grid.py | Computational Grid |
| FiniteDifferences.py | Spatial Discretization by Finite Differences |
| Time.py | Temporal Discretization |
| SolutionState.py | Container which stores the State of the lubricated contact |
| SolidsLibrary.py | Solid Material Properties Library |
| FluidLibrary.py | Liquid and Gas Material Properties Library |
| TwoPhaseModel.py | Cavitation Model |
| TriboContact.py | Greenwood-Tripp Asperity Contact Model & Wear Model |
| IOHDF5.py | Input/Output Routine Library |
| PostProcessing.py | Separate script to run Post-Processing |

Thereto follow the protocol below:

- i. Explore the different files and classes and understand their role, syntax and interaction.
- ii. **FiniteDifferences.py**: Implement the Finite Difference Discretization schemes and the corresponding sparse matrices, and verify them by means of a simple algebraic test function.
- iii. **ReynoldsSolver.py**: Implement an isothermal Reynolds' solver for the pressure field as described in Algorithm 1, excluding the squeeze term and temperature effects, i.e. ignore steps 8 \rightarrow 13. Use *scipy.sparse.linalg.spsolve()* to solve the linear system at a single iteration. Make sure the StateVector variables are updated at the end of the solver.
- iv. **Main.py** Write an outer time-loop in which you can validate the Reynolds' solver at a number of time steps, assuming a predefined minimum film thickness h_0 .
- v. **Main.py** Implement the intermediate Quasi-Newton method for satisfying the load balance per time step in order to determine the correct minimum film thickness h_0 .
- vi. **ReynoldsSolver.py**: Include the squeeze term in Reynolds' equation and verify.
- vii. **TriboContact.py**: Implement Contact Asperity model, using the predefined class-functions $I2()$ and $I52()$ for the special functions $F_2(\Lambda)$ and $F_{5/2}(\Lambda)$. Use for the calculation of the integrals *scipy.integral.quad()* routines. Test your implementation, and integrate it in the load-balance loop.
- viii. **ReynoldsSolver.py**: Implement the temperature equation in the solver and verify it.
- ix. **TriboContact.py**: Implement the wear model. Note that this can also be done off-line in the post-processing phase.

⁴Template code is based on Python 3.8.3 64-bit using Anaconda and Spyder 4 open-source software platform on windows 10.

2. Run the simulation for a complete combustion cycle, i.e. $\psi \in [0, 720^\circ]$, using a grid of $n_x = 256$ nodes and a time step of $5e - 5s$. The nominal temperature of the engine oil is assumed to be $T_{oil} = 95^\circ C$. Thereto, impose an under-relaxation-factor for pressure $\theta_P = 0.001$, for temperature $\theta_T = 0.01$ and for the film thickness $\theta_{h_0} = 0.25$. The convergence limit for pressure and temperature should be set to $Tol_P = Tol_T = 0.0001$ whereas that of the load balance can be put at $Tol_{h_0} = 0.001$.

Visualize, analyse, explain and report in a comprehensive way the computational results, i.e.

- i. Dimensionless Film Thickness evolution as function of ψ
- ii. The Stribeck curve, displaying the coefficient of friction versus the Hersey number.
- iii. Characteristic Pressure & Temperature fields at interesting and relevant locations.
- iv. Vapour Volume Fraction, Viscosity, Density,... at relevant locations.
- v. Velocity Field (e.g. 2D vector plot) at relevant locations.
- vi. Wear of Compression Ring and Wear at Cylinder liner after 1 combustion cycle.

Provide an motivated answer to following research questions

- i. Explain the sealing mechanism which prevents blow-by of combustion gasses to the carter. What is the role of the lubricant film in this process?
 - ii. What is the lifetime of the compression ring in terms of car mileage (km)? Assume thereto a constant engine speed of $2400rpm$ corresponding to a constant average car speed of $120km/h$. Assume further a constant wear rate over time and a maximum allowable reduction of the crown height of the ring to about 80%.
 - iii. What is the lifetime of the cylinder liner, of car mileage (km)? Assume a constant engine speed of $2400rpm$ corresponding to a constant average car speed of $120km/h$. Assume further a constant wear rate over time and a maximum wear groove depth in the cylinder liner of about $2\mu m$.
3. Consider in a second case, a worn compression ring with maximum crown height topped off at 75%. Perform a similar analysis as before. Compare the results with that of the first case and comment on the repercussions for the lubrication, pressure build-up, sealing, film thickness etc..
 4. Propose a specific measure to increase the energy efficiency and/or lower the wear, and support your claim by referring to literature and performing a simulation for validation in combination with a quantitative assessment of your hypothesis.
 5. Write down your analysis, observations, discussions and conclusions in a report of maximum15 pages.

A GEOMETRY AND PROPERTIES

| VW 2.0 R4 16v TDI CR 105kW | | |
|--|---------------------------------------|--------------------|
| Piston & Cylinder (Pearlitic Grey Cast Iron) | | |
| Bore D | 81 | mm |
| Stroke S | 95.5 | mm |
| Compression Ratio CR | 18 | |
| Cylinder Youngs Modulus E_c | 120 | GPa |
| Cylinder Hardness H_c | 250 | GPa |
| Cylinder Poisson Ratio ν_c | 0.28 | |
| Cylinder RMS roughness σ_c | 0.2 | μm |
| Connecting Rod Length l_r | 95.5 | mm |
| Crank Radius R_c | 47.75 | mm |
| Compression Ring (Nitrided Stainless Steel) | | |
| Height b | 1.5 | mm |
| Width w | 3.5 | mm |
| Crown Height δ | 10 | μm |
| Profile | $h_{prof} = 4 \frac{\delta x^2}{b^2}$ | |
| Free Gap Size $l_{gap,f}$ | 12 | mm |
| Gap Size l_{gap} | 0.5 | mm |
| Ring Youngs Modulus E_r | 210 | GPa |
| Ring Poisson Ratio ν_r | 0.28 | |
| Ring Hardness H_r | 1200 | GPa |
| RMS roughness σ_r | 0.1 | μm |
| Contact Conditions | | |
| Asperity Peak Density ζ | 97e9 | m^{-2} |
| Asperity Peak Average Radius of Curvature κ | 1.56 | μm |
| Eyring Shear Stress | 2 | MPa |
| Boundary shear strength coefficient f_b | 0.3 | |
| Dimensionless Wear Coefficient Ring k_r | $1.25e - 10$ | |
| Dimensionless Wear Coefficient Cylinder k_c | $2e - 10$ | |
| Operational Conditions | | |
| Atmospheric Inlet Pressure p_{atm} | 101325 | Pa |
| Engine RPM n | 2400 | rpm |
| Intake valve closing angle (IVC) | π | Degree Crank Angle |
| Start of combustion angle (SOC) | 2π | Degree Crank Angle |
| End of combustion angle (EOC) | $2\pi + \pi/4$ | Degree Crank Angle |
| Exhaust valve opening angle (EVO) | $3\pi - \pi/8$ | Degree Crank Angle |
| Adiabatic Expansion Coefficient γ | 1.35 | |
| Nominal Oil Temperature T_{oil} | 95 | $^{\circ}$ Celcius |
| Nominal Liner Temperature T_{wall} | 95 | $^{\circ}$ Celcius |

| SAE5W – 40 Lubricant Properties | | |
|---|---|----------|
| Liquid Dynamic Viscosity ν_l | $\mu_0 e^{\frac{B}{T-C}}$ | Pas |
| | $\mu_0 = 4.298e-5$ | Pas |
| | $B = 1285$ | K |
| | $C = 141.5$ | K |
| Liquid Density ρ_l | $\rho(T) = \frac{\rho_{ref}}{1+\beta(T(K)-T_{ref})}$ | kg/m^3 |
| | $T_{ref} = 100^\circ C, \quad \rho_{ref} = 804.5$ | kg/m^3 |
| Liquid Thermal Expansion | $\beta = 0.0007335$ | $1/K$ |
| Liquid Specific Heat Capacity $c_{p,l}$ | 1670 | J/kgK |
| Liquid Thermal Conductivity κ_l | 0.15 | W/mK |
| Liquid Speed of Sound c_l | 1461 | m/s |
| Liquid Limiting Shear stress τ_0 | 2 | MPa |
| Air-Vapour Properties | | |
| Vapour Dynamic Viscosity μ_v | $\mu_0 \left(\frac{T}{T_0}\right)^{3/2} \left(\frac{T_0+T_1}{T+T_1}\right)$ | Pas |
| | $\mu_0 = 1.716e-5$ | Pas |
| | $T_0 = 273.11$ | K |
| | $T_1 = 110.56$ | K |
| Vapour Density ρ_v | $\rho_v = \frac{p}{RT}, \quad R = 287.05 J/kgK$ | kg/m^3 |
| Vapour Specific Heat Capacity $c_{p,v}$ | 1008 | J/kgK |
| Vapour Thermal Conductivity κ_v | 0.03 | W/mK |
| Vapour Speed of Sound c_v | $\sqrt{1.4RT}$ | m/s |
| Mixture Properties | | |
| Saturation Pressure p_{sat} | 1e5 | Pa |
| Vapour Pressure p_{vap} | 1e3 | Pa |
| Vapour Volume Fraction $\alpha_s = \alpha(p_{sat})$ | 0.02 | |
| Vapour Volume Fraction $\alpha_v = \alpha(p_{vap})$ | 0.98 | |
| Mixture Density | $\rho(P, T) = \rho_l(1-\alpha) + \rho_v\alpha$ | kg/m^3 |
| Mixture Viscosity | $\mu(P, T) = \mu_l(1-\alpha) + \mu_v\alpha$ | Pas |
| Mixture Specific Heat | $c_p(P, T) = c_{p,l}(1-\alpha) + c_{p,v}\alpha$ | J/kgK |
| Mixture Thermal Conductivity | $\kappa(P, T) = \kappa_l(1-\alpha) + \kappa_v\alpha$ | W/mK |

B FINITE DIFFERENCE DISCRETIZATION

1st -order derivatives of a variable of interest f can be approximated in each node (x_i) of a Uniform Cartesian Computational Grid x with n_x nodes by one of following approximations, i.e. respectively 1st -order forward difference, 2nd -order central difference and 1st -order backward difference

$$\left. \frac{\partial f}{\partial x} \right|_i \approx \frac{f_{i+1} - f_i}{\Delta x}, \quad \forall i \in [1, n_x - 1] \quad (52)$$

$$\left. \frac{\partial f}{\partial x} \right|_i \approx \frac{f_{i+1} - f_{i-1}}{2\Delta x}, \quad \forall i \in [2, n_x - 1] \quad (53)$$

$$\left. \frac{\partial f}{\partial x} \right|_i \approx \frac{f_i - f_{i-1}}{\Delta x}, \quad \forall i \in [2, n_x] \quad (54)$$

Analogously 2nd -order derivatives of a variable of interest f can be approximated in each node (x_i) of a Uniform Cartesian Computational Grid x by one of following approximations, i.e. respectively 2nd -order forward difference, 2nd -order central difference and 2nd -order backward difference

$$\left. \frac{\partial^2 f}{\partial x^2} \right|_i \approx \frac{f_i - 2f_{i+1} + f_{i+2}}{\Delta x^2}, \quad \forall i \in [1, n_x - 2] \quad (55)$$

$$\left. \frac{\partial^2 f}{\partial x^2} \right|_i \approx \frac{f_{i+1} - 2f_i + f_{i-1}}{\Delta x^2}, \quad \forall i \in [2, n_x - 1] \quad (56)$$

$$\left. \frac{\partial^2 f}{\partial x^2} \right|_i \approx \frac{f_{i-2} - 2f_{i-1} + f_i}{\Delta x^2}, \quad \forall i \in [3, n_x] \quad (57)$$

For Reynolds equation, the more accurate central differences are preferable over the backward or forward difference, as they have no inherent numerical dissipation. However, at the domain boundaries, either the forward or backward approximation must be used in order to be able to evaluate the derivative.

In computational modelling, the (linear) discrete derivative of a function f is typically expressed as a $n_x \times n_x$ quasi-tri-diagonal linear system of equations, i.e.

$$\frac{\partial^k f}{\partial x^k} = \begin{bmatrix} d_1 & d_2 & d_3 & 0 & 0 & \dots & 0 \\ a & b & c & 0 & 0 & \dots & 0 \\ 0 & a & b & c & 0 & \dots & 0 \\ \vdots & \vdots & \vdots & \vdots & \vdots & \ddots & \vdots \\ 0 & \dots & 0 & a & b & c & 0 \\ 0 & \dots & \dots & 0 & a & b & c \\ 0 & \dots & \dots & \dots & d_{n_x-2} & d_{n_x-1} & d_{n_x} \end{bmatrix}^{n_x \times n_x} \cdot \begin{bmatrix} f_1 \\ f_2 \\ \vdots \\ f_{n_x} \end{bmatrix} \quad (58)$$

in which the coefficients a , b and c correspond to the finite difference coefficients of the 2nd -order central finite difference approximation and d_i correspond to those of the forward/backward approximation. If the values of f are known in each grid point x_i , one can evaluate derivatives of the function f immediately and explicitly.

However, when dealing with differential equations, the values of f are unknown and must comply the governing differential equation in each node, e.g.

$$\frac{\partial^k f}{\partial x^k} = RHS(x_i), \quad \forall i = [1..n_x] \quad (59)$$

subject to additional boundary conditions e.g. Dirichlet boundary conditions at $i = 1$ and $i = n_x$, yielding

$$f(x_1) = \alpha \quad (60)$$

$$f(x_{n_x}) = \beta \quad (61)$$

. In that case, the linear system becomes

$$\begin{bmatrix} 1 & 0 & 0 & 0 & 0 & \dots & 0 \\ a & b & c & 0 & 0 & \dots & 0 \\ 0 & a & b & c & 0 & \dots & 0 \\ \vdots & \vdots & \vdots & \vdots & \vdots & \ddots & \vdots \\ 0 & \dots & 0 & a & b & c & 0 \\ 0 & \dots & \dots & 0 & a & b & c \\ 0 & \dots & \dots & \dots & 0 & 0 & 1 \end{bmatrix}^{n_x \times n_x} \cdot \begin{bmatrix} f_1 \\ f_2 \\ \vdots \\ f_{n_x} \end{bmatrix} = \begin{bmatrix} \alpha \\ RHS_2 \\ RHS_3 \\ \vdots \\ RHS_{n_x-1} \\ \beta \end{bmatrix} \quad (62)$$

This linear system can be solve by using linear solvers such as Jacobi iteration, Gauss-Seidel, LU decomposition etc... Note that also Neumann boundary conditions can be implemented this way

In current assignment one should define the discretization matrices a priori, as sparse matrices⁵ by using the commands `A = scipy.sparse.diags(B,d,shape=(nx,nx),dtype='float',format='csr')`, which creates an $n_x \times n_x$ n-diagonal sparse matrix by taking the values of B and placing them along the diagonals specified by ds.

B.1 REYNOLDS EQUATION

Using the techniques above, the expanded Reynolds equation

$$\phi \frac{\partial^2 p}{\partial x^2} + \frac{\partial \phi}{\partial x} \frac{\partial p}{\partial x} = \frac{U}{2} \frac{\partial \rho h}{\partial x} + \frac{\partial \rho h}{\partial t}, \quad \phi = \frac{\rho h^3}{12\mu} \quad (63)$$

subject to Boundary Conditions

$$p\left(-\frac{b}{2}\right) = p_{carter} = 0 \quad (64)$$

$$p\left(\frac{b}{2}\right) = p_{cc}(\psi) - p_a \quad (65)$$

can be converted into following linear system

$$[M] \cdot [p] = [A + B] \cdot \begin{bmatrix} p_1 \\ p_2 \\ \vdots \\ p_{n_x} \end{bmatrix} = [RHS] \quad (66)$$

⁵Wiki: "In numerical analysis and scientific computing, a sparse matrix or sparse array is a matrix in which most of the elements are zero. By contrast, if most of the elements are non-zero, then the matrix is considered dense. When storing and manipulating sparse matrices on a computer, it is beneficial and often necessary to use specialized algorithms and data structures that take advantage of the sparse structure of the matrix. Operations using standard dense-matrix structures and algorithms are slow and inefficient when applied to large sparse matrices as processing and memory are wasted on the zeroes. Sparse data is by nature more easily compressed and thus requires significantly less storage. Some very large sparse matrices are infeasible to manipulate using standard dense-matrix algorithms."

in which

$$\begin{aligned}
 A &= \begin{bmatrix} \phi_1 & 0 & 0 & 0 & 0 & \dots & 0 \\ 0 & \phi_2 & 0 & 0 & 0 & \dots & 0 \\ 0 & 0 & \phi_3 & 0 & 0 & \dots & 0 \\ \vdots & \vdots & \vdots & \vdots & \vdots & \ddots & \vdots \\ 0 & \dots & 0 & 0 & \phi_{n_x-2} & 0 & 0 \\ 0 & \dots & \dots & 0 & 0 & \phi_{n_x-1} & 0 \\ 0 & \dots & \dots & \dots & 0 & 0 & \phi_{n_x} \end{bmatrix} \cdot \begin{bmatrix} \frac{1}{\Delta x^2} & -\frac{2}{\Delta x^2} & \frac{1}{\Delta x^2} & 0 & 0 & \dots & 0 \\ \frac{1}{\Delta x^2} & \frac{-2}{\Delta x^2} & \frac{1}{\Delta x^2} & 0 & 0 & \dots & 0 \\ 0 & \frac{1}{\Delta x^2} & \frac{-2}{\Delta x^2} & \frac{1}{\Delta x^2} & 0 & \dots & 0 \\ \vdots & \vdots & \vdots & \vdots & \vdots & \ddots & \vdots \\ 0 & \dots & 0 & \frac{1}{\Delta x^2} & \frac{-2}{\Delta x^2} & \frac{1}{\Delta x^2} & 0 \\ 0 & \dots & \dots & 0 & \frac{1}{\Delta x^2} & \frac{-2}{\Delta x^2} & \frac{1}{\Delta x^2} \\ 0 & \dots & \dots & 0 & \frac{1}{\Delta x^2} & -\frac{2}{\Delta x^2} & \frac{1}{\Delta x^2} \end{bmatrix} \\
 B &= \begin{bmatrix} \frac{\partial \phi}{\partial x} 1 & 0 & 0 & 0 & 0 & \dots & 0 \\ 0 & \frac{\partial \phi}{\partial x} 2 & 0 & 0 & 0 & \dots & 0 \\ 0 & 0 & \frac{\partial \phi}{\partial x} 3 & 0 & 0 & \dots & 0 \\ \vdots & \vdots & \vdots & \vdots & \vdots & \ddots & \vdots \\ 0 & \dots & 0 & 0 & \frac{\partial \phi}{\partial x} n_x-2 & 0 & 0 \\ 0 & \dots & \dots & 0 & 0 & \frac{\partial \phi}{\partial x} n_x-1 & 0 \\ 0 & \dots & \dots & \dots & 0 & 0 & \frac{\partial \phi}{\partial x} n_x \end{bmatrix} \cdot \begin{bmatrix} \frac{1}{\Delta x} & -\frac{1}{\Delta x} & 0 & 0 & 0 & \dots & 0 \\ -\frac{1}{2\Delta x} & 0 & \frac{1}{2\Delta x} & 0 & 0 & \dots & 0 \\ 0 & -\frac{1}{2\Delta x} & 0 & \frac{1}{2\Delta x} & 0 & \dots & 0 \\ \vdots & \vdots & \vdots & \vdots & \vdots & \ddots & \vdots \\ 0 & \dots & 0 & -\frac{1}{2\Delta x} & 0 & \frac{1}{2\Delta x} & 0 \\ 0 & \dots & \dots & 0 & -\frac{1}{2\Delta x} & 0 & \frac{1}{2\Delta x} \\ 0 & \dots & \dots & \dots & 0 & -\frac{1}{\Delta x} & \frac{1}{\Delta x} \end{bmatrix} \\
 RHS = \frac{U}{2} &= \begin{bmatrix} \frac{1}{\Delta x} & -\frac{1}{\Delta x} & 0 & 0 & 0 & \dots & 0 \\ -\frac{1}{2\Delta x} & 0 & \frac{1}{2\Delta x} & 0 & 0 & \dots & 0 \\ 0 & -\frac{1}{2\Delta x} & 0 & \frac{1}{2\Delta x} & 0 & \dots & 0 \\ \vdots & \vdots & \vdots & \vdots & \vdots & \ddots & \vdots \\ 0 & \dots & 0 & -\frac{1}{2\Delta x} & 0 & \frac{1}{2\Delta x} & 0 \\ 0 & \dots & \dots & 0 & -\frac{1}{2\Delta x} & 0 & \frac{1}{2\Delta x} \\ 0 & \dots & \dots & \dots & 0 & -\frac{1}{\Delta x} & \frac{1}{\Delta x} \end{bmatrix} \cdot \begin{bmatrix} \rho_1 h_1 \\ \rho_2 h_2 \\ \rho_3 h_3 \\ \vdots \\ \rho_{n_x-2} h_{n_x-2} \\ \rho_{n_x-1} h_{n_x-1} \\ \rho_{n_x} h_{n_x} \end{bmatrix} + \begin{bmatrix} \frac{\rho_2^t h_1^t - \rho_2^{t-1} h_1^{t-1}}{\Delta t} \\ \frac{\rho_2^t h_2^t - \rho_2^{t-1} h_2^{t-1}}{\Delta t} \\ \frac{\rho_3^t h_3^t - \rho_3^{t-1} h_3^{t-1}}{\Delta t} \\ \vdots \\ \frac{\rho_{n_x-2}^t h_{n_x-2}^t - \rho_{n_x-2}^{t-1} h_{n_x-2}^{t-1}}{\Delta t} \\ \frac{\rho_{n_x-1}^t h_{n_x-1}^t - \rho_{n_x-1}^{t-1} h_{n_x-1}^{t-1}}{\Delta t} \\ \frac{\rho_{n_x}^t h_{n_x}^t - \rho_{n_x}^{t-1} h_{n_x}^{t-1}}{\Delta t} \end{bmatrix}
 \end{aligned}$$

In the matrix notations above, first-order finite difference approximations have been used for the derivatives at the boundaries, instead of imposing immediately Dirichlet and Neumann the boundary conditions. This allows to pre-define finite difference matrices in the class **FiniteDifferences**. The boundary conditions should be imposed on the composite matrix M and RHS, as follows

$$\begin{aligned}
 M[0,0] &= 1, & M[0,2:n_x-1] &= 0 \\
 M[n_x-1,n_x-1] &= 1, & M[n_x-1,1:n_x-2] &= 0 \\
 RHS[0] &= p_{cart} - p_a \\
 RHS[n_x-1] &= p_{cc}(\psi) - p_a
 \end{aligned}$$

This operation can be done efficiently with the functions **SetDirichletLeft(M)** and **SetDirichletRight(M)** from the finite difference class. This nonlinear system is solved iteratively using a linear solver. In order to guarantee numerical stability and convergence, we apply following under-relaxation method to obtain the pressure at iteration $k+1$

$$p^* = [M]^{-1} [RHS] \quad (67)$$

$$\Delta p = \max(p^*, 0) - p^k \quad (68)$$

$$p^{k+1} = p^k + \theta_P \Delta p, \quad 0 < \theta_P \leq 1 \quad (69)$$

B.2 TEMPERATURE EQUATION

The 1D transport equation for the temperature averaged over the film thickness, i.e.

$$\frac{\partial \bar{T}}{\partial t} + \bar{u} \frac{\partial \bar{T}}{\partial x} - \frac{\kappa}{\rho c_p} \frac{\partial^2 \bar{T}}{\partial x^2} = \frac{1}{\rho c_p} \bar{Q} \quad (70)$$

is a so called hyperbolic partial differential equation. This equation is supplemented by following boundary conditions

$$U > 0 \quad \left\{ \begin{array}{l} \frac{\partial T}{\partial x} \left(\frac{b}{2} \right) = 0 \\ T \left(-\frac{b}{2} \right) = T_{oil} \end{array} \right. \quad (71)$$

$$U \leq 0 \quad \left\{ \begin{array}{l} T \left(\frac{b}{2} \right) = T_{oil} \\ \frac{\partial T}{\partial x} \left(-\frac{b}{2} \right) = 0 \end{array} \right. \quad (72)$$

The temperature equation requires a so-called *Upwind discretization* of the LHS convective term, in order to guarantee numerical stability. The upwind discretization is in principle equivalent with a first-order forward or backward finite difference scheme. However, the choice for using forward or backward discretization is determined by the sign of the flow velocity. The aim is to use only the 'information' for the discretization upstream of the flow direction, such that a stable propagation of the temperature field is obtained.

$$\bar{u} \frac{\partial T}{\partial x} \bigg|_i \approx \bar{u}_i \frac{T_i - T_{i-1}}{\Delta x}, \quad \text{if } \bar{u}_i > 0 \quad (73)$$

$$\bar{u} \frac{\partial T}{\partial x} \bigg|_i \approx \bar{u}_i \frac{T_{i+1} - T_i}{\Delta x}, \quad \text{if } \bar{u}_i < 0 \quad (74)$$

To obtain the $k + 1$ -th approximation of the temperature at the current time step t , the 1D temperature equation is solved using a stable implicit scheme as

$$T^* = [M]^{-1} [RHS_T] \quad (75)$$

$$\Delta T = T^* - T^{t,k} \quad (76)$$

$$T^{t,k+1} = T^{t,k} + \theta_T \Delta T, \quad 0 < \theta_T \leq 1 \quad (77)$$

in which $M = I + D + E$. The identity matrix I is defined here as

$$I = \begin{bmatrix} 1 & 0 & 0 & 0 & 0 & \dots & 0 \\ 0 & 1 & 0 & 0 & 0 & \dots & 0 \\ 0 & 0 & 1 & 0 & 0 & \dots & 0 \\ \vdots & \vdots & \vdots & \vdots & \vdots & \ddots & \vdots \\ 0 & \dots & 0 & 0 & 1 & 0 & 0 \\ 0 & \dots & \dots & 0 & 0 & 1 & 0 \\ 0 & \dots & \dots & \dots & 0 & 0 & 1 \end{bmatrix} \quad (78)$$

Defining $\bar{u}^+(x) = \max(\bar{u}(x), 0)$ and $\bar{u}^-(x) = \min(\bar{u}(x), 0)$, the matrices E and D are given by

$$\begin{aligned}
 D &= \begin{bmatrix} \bar{u}_1^+ \Delta & 0 & 0 & 0 & 0 & \dots & 0 \\ 0 & \bar{u}_2^+ \Delta t & 0 & 0 & 0 & \dots & 0 \\ 0 & 0 & \ddots & 0 & 0 & \dots & 0 \\ \vdots & \vdots & \vdots & \vdots & \vdots & \ddots & \vdots \\ 0 & \dots & 0 & 0 & \ddots & 0 & 0 \\ 0 & \dots & \dots & 0 & 0 & \bar{u}_{n_x-1}^+ \Delta t & 0 \\ 0 & \dots & \dots & \dots & 0 & 0 & \bar{u}_{n_x}^+ \Delta t \end{bmatrix} \cdot \begin{bmatrix} -\frac{1}{\Delta x} & \frac{1}{\Delta x} & 0 & 0 & 0 & \dots & 0 \\ -\frac{1}{\Delta x} & \frac{1}{\Delta x} & 0 & 0 & 0 & \dots & 0 \\ 0 & -\frac{1}{\Delta x} & \frac{1}{\Delta x} & 0 & 0 & \dots & 0 \\ \vdots & \vdots & \vdots & \vdots & \vdots & \ddots & \vdots \\ 0 & \dots & 0 & -\frac{1}{\Delta x} & \frac{1}{\Delta x} & 0 & 0 \\ 0 & \dots & \dots & 0 & -\frac{1}{\Delta x} & \frac{1}{\Delta x} & 0 \\ 0 & \dots & \dots & \dots & 0 & -\frac{1}{\Delta x} & \frac{1}{\Delta x} \end{bmatrix} \\
 &+ \begin{bmatrix} \bar{u}_1^- \Delta t & 0 & 0 & 0 & 0 & \dots & 0 \\ 0 & \bar{u}_2^- \Delta t & 0 & 0 & 0 & \dots & 0 \\ 0 & 0 & \ddots & 0 & 0 & \dots & 0 \\ \vdots & \vdots & \vdots & \vdots & \vdots & \ddots & \vdots \\ 0 & \dots & 0 & 0 & \ddots & 0 & 0 \\ 0 & \dots & \dots & 0 & 0 & \bar{u}_{n_x-1}^- \Delta t & 0 \\ 0 & \dots & \dots & \dots & 0 & 0 & \bar{u}_{n_x}^- \Delta t \end{bmatrix} \cdot \begin{bmatrix} -\frac{1}{\Delta x} & \frac{1}{\Delta x} & 0 & 0 & 0 & \dots & 0 \\ 0 & -\frac{1}{\Delta x} & \frac{1}{\Delta x} & 0 & 0 & \dots & 0 \\ 0 & 0 & -\frac{1}{\Delta x} & \frac{1}{\Delta x} & 0 & \dots & 0 \\ \vdots & \vdots & \vdots & \vdots & \vdots & \ddots & \vdots \\ 0 & \dots & 0 & 0 & -\frac{1}{\Delta x} & \frac{1}{\Delta x} & 0 \\ 0 & \dots & \dots & 0 & 0 & -\frac{1}{\Delta x} & \frac{1}{\Delta x} \\ 0 & \dots & \dots & \dots & 0 & -\frac{1}{\Delta x} & \frac{1}{\Delta x} \end{bmatrix} \\
 E &= - \begin{bmatrix} \frac{\Delta t \kappa}{\rho c_p \ 1} & 0 & 0 & 0 & 0 & \dots & 0 \\ 0 & \frac{\Delta t \kappa}{\rho c_p \ 2} & 0 & 0 & 0 & \dots & 0 \\ 0 & 0 & \frac{\Delta t \kappa}{\rho c_p \ 3} & 0 & 0 & \dots & 0 \\ \vdots & \vdots & \vdots & \vdots & \vdots & \ddots & \vdots \\ 0 & \dots & 0 & 0 & \frac{\Delta t \kappa}{\rho c_p \ n_x-2} & 0 & 0 \\ 0 & \dots & \dots & 0 & 0 & \frac{\Delta t \kappa}{\rho c_p \ n_x-1} & 0 \\ 0 & \dots & \dots & \dots & 0 & 0 & \frac{\Delta t \kappa}{\rho c_p \ n_x} \end{bmatrix} \cdot \begin{bmatrix} \frac{1}{\Delta x^2} & -\frac{2}{\Delta x^2} & \frac{1}{\Delta x^2} & 0 & 0 & \dots & 0 \\ \frac{1}{\Delta x^2} & -\frac{2}{\Delta x^2} & \frac{1}{\Delta x^2} & 0 & 0 & \dots & 0 \\ 0 & \frac{1}{\Delta x^2} & -\frac{2}{\Delta x^2} & \frac{1}{\Delta x^2} & 0 & \dots & 0 \\ \vdots & \vdots & \vdots & \vdots & \vdots & \ddots & \vdots \\ 0 & \dots & 0 & \frac{1}{\Delta x^2} & -\frac{2}{\Delta x^2} & \frac{1}{\Delta x^2} & 0 \\ 0 & \dots & \dots & 0 & \frac{1}{\Delta x^2} & -\frac{2}{\Delta x^2} & \frac{1}{\Delta x^2} \\ 0 & \dots & \dots & 0 & \frac{1}{\Delta x^2} & -\frac{2}{\Delta x^2} & \frac{1}{\Delta x^2} \end{bmatrix}
 \end{aligned}$$

$$RHS_T = \begin{bmatrix} T_1^{t-1} \\ T_2^{t-1} \\ T_3^{t-1} \\ \vdots \\ T_{n_x-2}^{t-1} \\ T_{n_x-1}^{t-1} \\ T_{n_x}^{t-1} \end{bmatrix} + \begin{bmatrix} \left. \frac{\Delta t \bar{Q}^{t,k}}{\rho^{t,k} c_p^{t,k}} \right|_1 \\ \left. \frac{\Delta t \bar{Q}^{t,k}}{\rho^{t,k} c_p^{t,k}} \right|_2 \\ \left. \frac{\Delta t \bar{Q}^{t,k}}{\rho^{t,k} c_p^{t,k}} \right|_3 \\ \vdots \\ \left. \frac{\Delta t \bar{Q}^{t,k}}{\rho^{t,k} c_p^{t,k}} \right|_{n_x-2} \\ \left. \frac{\Delta t \bar{Q}^{t,k}}{\rho^{t,k} c_p^{t,k}} \right|_{n_x-1} \\ \left. \frac{\Delta t \bar{Q}^{t,k}}{\rho^{t,k} c_p^{t,k}} \right|_{n_x} \end{bmatrix} \quad (79)$$

in which the shear heating \bar{Q} at the right-hand side is given by expression (23). Analogously to Reynolds equation, the boundary conditions have to be (re)set after construction of the matrix system.

For $U \leq 0$ boundary conditions are

$$\begin{aligned} M[0, 0 : 1] &= \left[\frac{-1}{\Delta x}, \frac{1}{\Delta x} \right], \quad M[0, 3 : n_x - 1] = 0 \\ M[n_x - 1, n_x - 1] &= 1, \quad M[n_x - 1, 1 : n_x - 2] = 0, \\ RHS_T[0] &= 0 \\ RHS_T[n_x - 1] &= T_{oil} \end{aligned}$$

For $U > 0$ boundary conditions are

$$\begin{aligned} M[0, 0] &= 1, \quad M[2 : n_x - 1, 0] = 0 \\ M[n_x - 1, n_x - 2 : n_x - 1] &= \left[\frac{-1}{\Delta x}, \frac{1}{\Delta x} \right], \quad M[n_x - 1, 1 : n_x - 3] = 0 \\ RHS_T[0] &= T_{oil} \\ RHS_T[n_x - 1] &= 0 \end{aligned}$$